

Ductile–brittle behavior of (001)[110] nano-cracks in bcc iron

Anna Machová^{a,*}, Glenn E. Beltz^b

^a Institute of Thermomechanics AS CR, 18200 Prague 8, Dolejškova 5, Czech Republic

^b Department of Mechanical and Environmental Engineering, University of California, Santa Barbara, CA 93106-5070, USA

Received 25 August 2003; received in revised form 13 November 2003

Abstract

We carry out atomistic simulations and stress analysis of crack behavior in bcc iron under Mode I, quasi-static loading. We observe that the formation of unstable stacking faults at the crack tip of a relatively long crack (~ 16 nm) cannot prevent unstable crack extension at the Griffith level. A crack of smaller dimensions (~ 4 nm) produces twinning on the $\langle 111 \rangle \{112\}$ slip system ahead of the tip, which gives rise to a slow ductile growth during subsequent quasi-static loading. The influence of the T-stress on the shear processes at the crack tip and crack stability is discussed.

© 2004 Elsevier B.V. All rights reserved.

Keywords: Crack growth; Twinning; bcc iron

1. Introduction

Atomistic simulations (e.g. [1,2]) show that the ductile versus brittle response of cracks under plane strain conditions depends on the relative orientation of the crack plane and available slip systems. If the active slip system in bcc iron is considered to be $\langle 111 \rangle \{112\}$, then generally three different shear processes may be observed at a crack tip under plane strain conditions: generation of extrinsic stacking faults, twinning, or emission of edge dislocations. Atomistic simulations indicate that these different shear processes have different consequences for the stability of nano-cracks in bcc iron, which may influence the embrittlement of ferritic steels. For that reason, the topic has been recently studied in bcc iron both via continuum [3,4] and atomistic methods [4–6]. Dislocation emission on the $\langle 111 \rangle \{112\}$ type slip systems and stability of $(\bar{1}10)[110]$ cracks were recently studied by Beltz and Machová [4]. Generation of unstable stacking faults and twinning on the same type of slip system and crystal orientation were studied for (001)[110] cracks by Machová et al. [5]. Kinetic and acoustic emission during growth of defects are analyzed by Landa et al. [6].

In this paper, we focus on the stability of (001)[110] nano-cracks, where the available slip systems $\langle 111 \rangle \{112\}$ are oriented in the “easy” twinning direction and inclined with respect to the crack plane at an angle $\theta \approx 35^\circ$. The behavior of the (001) cracks is compared with the $(\bar{1}10)[110]$ cracks, where the available slip systems $\langle 111 \rangle \{112\}$ are oriented in the “hard” (anti-twinning) direction at an inclination of $\theta \approx 55^\circ$. We use molecular dynamic (MD) simulations with an N-body potential described by Machová and Ackland [7] and continuum mechanics based on the Rice framework [8] in perfect and cracked samples to understand the critical behavior of the aforementioned cracks loaded in Mode I.

2. MD simulations

A central pre-existing crack is considered in an initially rectangular crystal. The relatively large crystals are oriented along the axes $x_1 = [\bar{1}10]$, $x_2 = [001]$, and $x_3 = [110]$. The crack faces are coincident with (001) planes, and the crack front is oriented along the [110] direction. Plane strain conditions in the x_3 direction are considered (i.e. $\varepsilon_{33} = \varepsilon_{32} = \varepsilon_{31} = 0$). Due to the symmetry of the problem, we treat only one half of the sample in the simulations. Crack simulations are performed by a molecular dynamic technique, where thermal atomic motion of individual atoms

* Corresponding author. Tel.: +420 2 660 53 023; fax: +420 2 858 4695.

E-mail address: machova@it.cas.cz (A. Machová).

is not controlled, similar to earlier work by Machová and coworkers [5–7]. Prior to external loading, the samples are relaxed to avoid the influence of atomic surface relaxations on crack tip processes. Then, the sample is loaded gradually in far-field uniaxial tension up to a level σ_A . When the prescribed level is reached, the applied stress is held constant (as in Fig. 3 in [5]). The (001)[110] cracks are loaded during 4000 time integration steps, while the $(\bar{1}10)[110]$ cracks are loaded during 6000 time integration steps of magnitude 10^{-14} s. The kinetic energy in the system during the loading is very small (see e.g. Fig. 15 in [5]). This effectively implies that the external loading is quasi-static, and that the average temperature in the entire sample is close to 0 K, consistent with the continuum models advanced in [3,4].

The (001) cracks are embedded in a sample containing 400 atomic planes in the x_2 -direction and 200 planes in the x_1 -direction. The half crack length of the longer crack corresponds to $l_o = 80 d_{110}$, while for the smaller crack, it is $l_o = 20 d_{110}$, where $d_{110} = a_o/\sqrt{2}$ is the interplanar distance between the $\{110\}$ planes and $a_o = 2.8665 \text{ \AA}$ is the lattice parameter in iron. The boundary correction factor F_I for the longer crack is 1.4, while for the smaller crack, it is approximately unity; the correction factor is defined such that the stress intensity factor is adequately approximated by $F_I \sigma(\pi l_o)^{1/2}$ [9].

Besides monitoring the global energy balance, the total number of interactions, and the local interactions at the crack tip, we also calculate stress on the atomic level [10]. We use the concept of interplanar stress [8], since the interplanar stresses are capable of satisfactorily describing the local stress if an inhomogeneous strain distribution appears within the range of interatomic interaction. The topic is important for modeling of dislocation emission and the formation of new surfaces or interfaces.

3. Results and discussion

Comparison of the LEFM solution with the MD results under a relatively small applied stress $\sigma_A = 1.364 \text{ GPa}$ (elastic static regime) is shown in Fig. 1 for the longer crack $l_o = 80 d_{110}$. It is seen that the normal near stress field $\sigma_2 = K_{IA}/(2\pi r)^{1/2}$ in front of the crack tip is well described by the stress intensity factor $K_{IA} = F_I \sigma_A (\pi l_o)^{1/2}$, with $F_I = 1.4$. This supports our use of the stress intensity factor K to describe the loading level in our atomistic simulations.

Under the gradual quasi-static loading up to larger stress, the longer crack ($80 d_{110}$) begins to propagate at an applied stress $\sigma_A = 2.74 \text{ GPa}$, which corresponds to the stress intensity factor $K_{IA} = 0.87 \text{ MPa m}^{1/2}$. Crack growth initiated at time step 4028, shortly after the constant level of the applied stress had been reached. The profile of the normal stress σ_{22} in the MD at crack initiation is shown in Fig. 2. Cracking is initiated when the work done by the normal stress at the crack tip ($W_{001} = 3.815 \text{ J/m}^2$) exceeded the theoretical value $2\gamma_s = 3.624 \text{ J/m}^2$ needed for formation of new

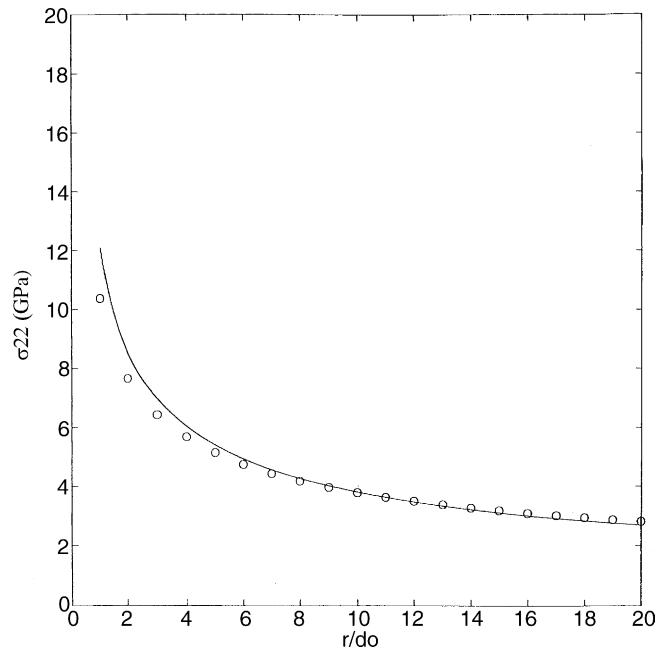


Fig. 1. The near-tip stress field (σ_{22}) given by linear elastic fracture mechanics (solid line) and our MD results (circles) in front of the crack tip for a crack size $l_o = 80 d_{110}$. The (001)[110] crack is loaded in Mode I, with $K_{IA} = 0.43 \text{ MPa m}^{1/2}$.

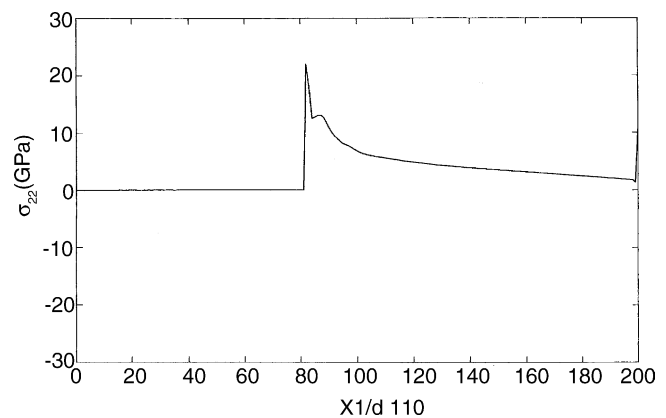


Fig. 2. The stress component σ_{22} from our MD simulations on the mid-plane of the sample at the initiation of the crack propagation ($l_o = 80 d_{110}$).

free (001) surfaces via cleavage [7]. The theoretical Griffith stress intensity K_G in an anisotropic medium needed for cleavage is given by the relation $2\gamma_s = C(A_{ij})K_G^2$, where for our crack orientation, the anisotropic constant is $C(A_{ij}) = 4.367 \times 10^{-12} \text{ m}^2/\text{N}$ and $K_G = 0.91 \text{ MPa m}^{1/2}$.¹ Crack extension at a stress intensity $K_{IA} = 0.96 K_G$ and time step

¹ The values $C(A_{ij})$ and K_G differ slightly from those used in [7] since we have used here a new set of constants A_{ij} that suitably describe the stress-strain relations under plane strain in both the [001] and [110] directions. The new constants are $A_{11} = 0.4470$, $A_{12} = -0.2664$, $A_{22} = 0.5698$, and $A_{66} = 0.8621 \times 10^{-11} \text{ m}^2/\text{N}$. The constants A_{ij} given in [7] describe the relations solely in the [001] direction. This change influences the value of K_G by less than by 5%.

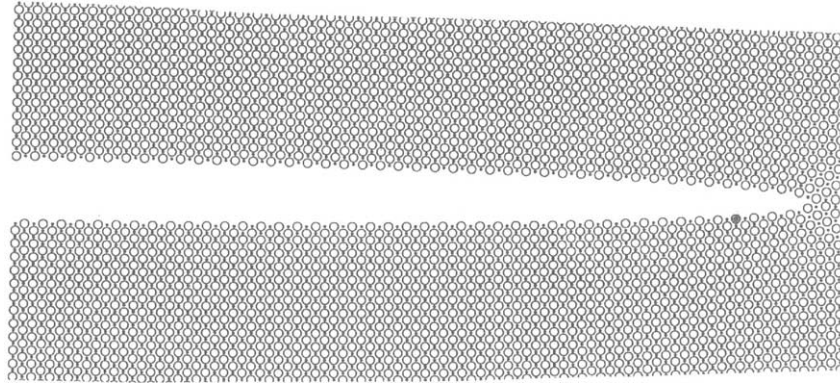


Fig. 3. Crack extension at time step 4500 with $K_{IA} = 0.96K_G$. The original crack tip atom of the crack (size $l_o = 80 d_{110}$) is denoted in black.

4500 is depicted in Fig. 3. The initial velocity of crack extension corresponds to about 400 m/s. Crack initiation is accompanied by the generation of an unstable three-layer stacking fault (3SF) at the crack tip, causing some shielding evident in Fig. 2. When the original crack tip atoms become surface atoms subsequent to crack advance, the unstable defects are unloaded and vanish at free crack faces (Fig. 4). This quasi-brittle behavior at the Griffith level is applicable to longer cracks loaded in the elastic regime.

However, if a (001)[110] crack of smaller dimension ($l_o = 20 d_{110}$) is loaded quasi-statically in the nonlinear region at a sufficiently high stress, twinning at the crack tip on the $\langle 111 \rangle \{112\}$ slip system, accompanied by just a very slow, subcritical crack growth (abetted by twinning) is observed in the MD simulations at $K_{IA} = 0.83K_G$ (see Fig. 5). Consideration of “perfect” (that is, uncracked) samples reveals that the above mentioned behavior is attributable to the fact that shear processes occur in the easy twinning direction, where the peak stress for ideal twin formation ($\tau_{\text{twin}} = 9.3$ GPa) is lower than for dislocation generation ($\tau_{\text{disl}} = 16.3$ GPa) [5]. This is also in qualitative agreement with continuum modeling of stacking fault formation at a crack tip by

Chang [3]. Fig. 5 also suggests that twinning at the crack tip may represent one mechanism of a subcritical ductile crack growth. Consistent with experimental observations, the MD results also show (Fig. 6) that crack nucleation in bcc iron may occur at twin intersections.

The maximum shear stress observed in the MD simulations during twin formation at the small crack ($l_o = 20 d_{110}$) occurs at time step 2500 and corresponds to about 6.15 GPa, which is less than τ_{twin} . However, the energy and peak stress needed for twin formation can be reduced via the T-stress (a stress component acting along the axis of crack extension in excess of what is described by the K-field), similar to dislocation generation at a crack [4], or similar to the formation of a plastic zone at the crack tip in an elastic/plastic medium analyzed by Rice [11]. A rough (isotropic) estimate for our crack geometries can be performed utilizing the compendium of T-stress solutions from [12] and the model by Rice, where the critical shear stress τ_c in a slip system inclined with respect to the crack plane under an angle θ is reduced via a simple interchange $\tau_c \rightarrow \tau_c + T \sin\theta \cos\theta$. The T-stress from [12] is given by the relation $T = \lambda\sigma_A(1 - a/W)$, where $a = l_o$, $W = 200 d_{110}$, and the constant λ differs for the different crack geometries. For the smaller crack ($l_o = 20 d_{110}$) the relevant values are: $\sigma_A = 4.80$ GPa [5], $a/W = 0.1$, $\lambda = -0.93$, $\sin\theta \cos\theta = 0.47$, which gives $T = -4.02$ GPa and reduces the critical shear stress for twin formation to $\tau_c = 7.4$ GPa, close to the value 6.15 GPa observed in MD.

The maximum shear stress observed in the MD simulations for the longer crack ($l_o = 80 d_{110}$) is 5.5 GPa. The geometry and load are different: $a/W = 0.4$, $\lambda = -0.79$, and $\sigma_A = 1.71$ GPa, which gives $T = -0.81$ GPa. Due to the T value, the reduction of the critical shear stress needed for twin formation is small: $\tau_c = 8.92$ GPa, which is far from the MD peak of 5.5 GPa. The smaller shear stress apparent in the MD simulation is not sufficient for twinning. This explains why twin formation does not occur at the longer (001) crack and indicates that the small negative or zero values of the T-stress support brittle behavior of cracks. (We have verified that the T-stress by Fett [12] adequately de-

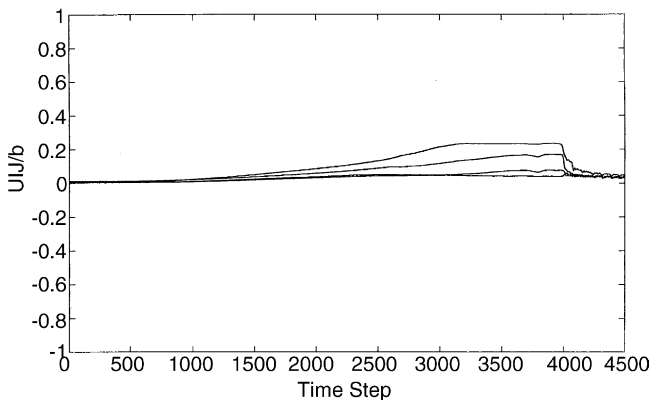


Fig. 4. Relative shear displacements at the crack tip on the $\langle 111 \rangle \{112\}$ slip system between the first (upper curve), the second, and the third neighboring plane disappear after initiation (time step 4028) of the crack (size $l_o = 80 d_{110}$).

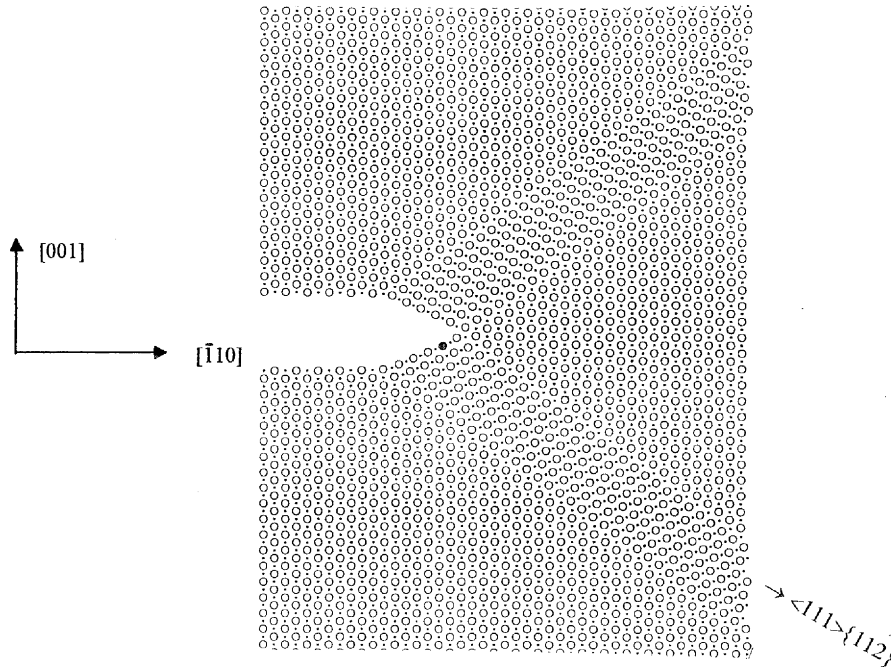


Fig. 5. Twinning at the crack tip of the crack (size $l_o = 20 d_{110}$), at time step 3500, with $K_{IA} = 0.83K_G$. The original crack tip point is denoted in black.

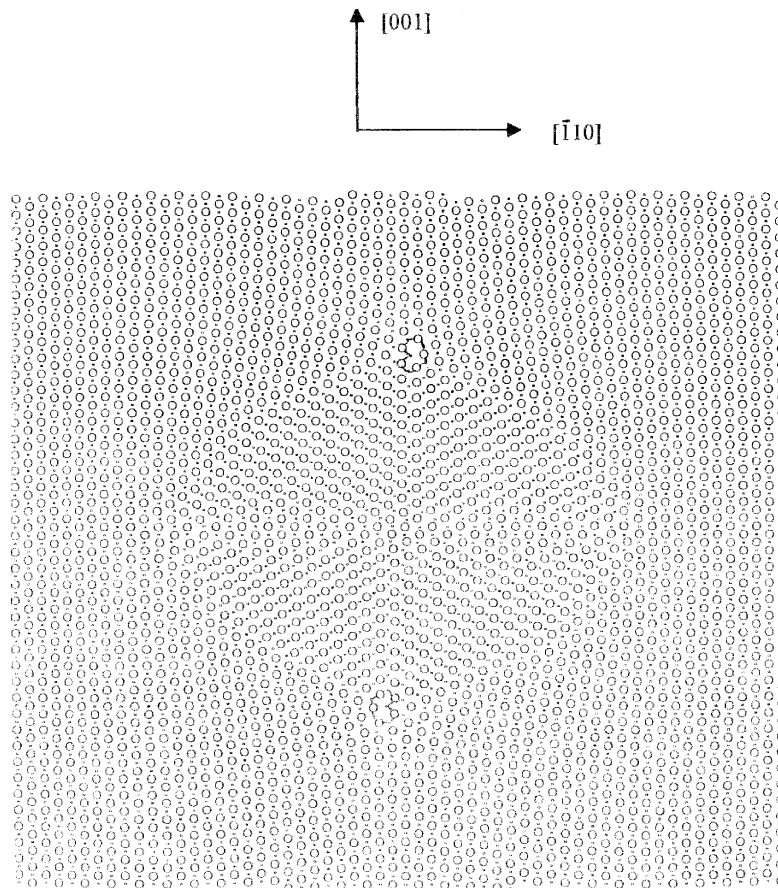


Fig. 6. Detail of crack nucleation at twin intersection in a perfect sample loaded by a pressure of 35 GPa in the (001) direction.

scribes the stress component σ_{11} near the crack tip in the MD simulations.)

Dislocation generation in the $\langle 111 \rangle \{112\}$ slip systems in perfect samples is favored in the difficult anti-twinning direction, since here the peak stress for dislocation formation ($\tau_{\text{disl}} = 16.3$ GPa) is lower than for twin formation ($\tau_{\text{twin}} = 27.9$ GPa). We note that this is in qualitative agreement with the results by Vitek [13] and Paidar [14]. This was also confirmed in our MD simulations with a different crack orientation $(-110)[110]$. Since these cracks emit complete edge dislocations causing crack tip blunting, the cracks $(-110)[110]$ were stable under a pure Mode I loading. Here, the ductile–brittle transition at the crack tip can be observed under biaxial loading [4] when the T-stress approaches zero or positive values.

4. Conclusion

Our results indicate that nano-cracks on (001) planes in iron with the available slip systems $\langle 111 \rangle \{112\}$ oriented in the easy twinning direction can be unstable. The response can be either cleavage, or cracking accompanied by twinning. The crack size effect can be understood in terms of the T-stress: for a uniaxial loading, short cracks possess a T-stress of larger magnitude and thus are more susceptible to twinning behavior. The atomistic results are in agreement with experimental observations that brittle fracture in bcc iron is observed only on $\{100\}$ type planes.

Acknowledgements

The work was supported by the National Science Foundation under award number CMS-0000142 and Czech Science Foundation under grants A2076201, AV0Z2076919, and ME 504. The authors thank Margherita Chang and Zdeňek Rosecký for their cooperation.

References

- [1] S. Kohlhoff, P. Gumbsch, H.F. Fischmeister, *Phil. Mag. A* 64 (1991) 851.
- [2] V. Shastry, D. Farkas, *Model. Simul. Mater. Sci. Eng.* 4 (1996) 473.
- [3] M. Chang, *Multi-Scale Multi-Plane Model for Stacking Fault and Twinning Formation in bcc Iron*, PhD Thesis, University of California, Santa Barbara, 2002.
- [4] G.E. Beltz, A. Machová, *Scripta Materialia* 50 (2004) 483.
- [5] A. Machová, G.E. Beltz, M. Chang, *Model. Simul. Sci. Eng.* 7 (1999) 949.
- [6] M. Landa, J. Cerv, A. Machová, Z. Rosecký, *J. Acoust. Emission* 20 (2002) 25.
- [7] A. Machová, G.J. Ackland, *Model. Simul. Mater. Sci. Eng.* 6 (1998) 521.
- [8] J.R. Rice, *J. Mech. Phys. Solids* 40 (1992) 239.
- [9] Y. Murakami, *Stress Intensity Factor Handbook*, vol. 1, Pergamon Press, Oxford, 1987, p. 67.
- [10] A. Machová, *Model. Simul. Mater. Sci. Eng.* 9 (2001) 327.
- [11] J.R. Rice, *J. Mech. Phys. Solids* 22 (1974) 17.
- [12] T. Fett, *A compendium of T-stress solutions*, Research report FZKA 6057, Forschungszentrum Karlsruhe GmbH, 1998, p. 32.
- [13] V. Vitek, *Scripta Metall.* 4 (1970) 725.
- [14] V. Paidar, *Phil. Mag. A* 48 (1983) 231.